POTENTIAL-FIELD-BASED ACTIVE EXPLORATION FOR ACOUSTIC SIMULTANEOUS LOCALIZATION AND MAPPING

Christopher Schymura and Dorothea Kolossa

Institute of Communication Acoustics, Ruhr-Universität Bochum, Germany

ABSTRACT

This paper presents a novel framework for active exploration in the context of acoustic simultaneous localization and mapping (SLAM) using a microphone array mounted on a mobile robotic agent. Acoustic SLAM aims at building a map of acoustic sources present in the environment and simultaneously estimating the agent's own trajectory and position within this map. Two important aspects of this task are robustness against disturbances arising from reverberation and sensor imperfections and an appropriate degree of exploration to achieve high map accuracy. Several approaches to the latter aspect using information-theoretic measures have recently been proposed. This study extends these approaches into a framework based on the potential field method, which is a widely used technique for robotic path planning and navigation. It allows to determine exploratory movement trajectories for the robotic agent via gradient descent, without requiring computationally expensive Monte Carlo simulations to predict the effects of specific trajectory choices. Furthermore, additional constraints like maintaining a safe distance to acoustic sources can easily be integrated into this framework. Experimental evaluation demonstrates that the proposed method yields adequate exploration strategies of the acoustic environment leading to accurate map estimates.

Index Terms— acoustic simultaneous localization and mapping, robot audition, potential field method

1. INTRODUCTION

The problem of acoustic scene mapping (ASM) has recently become a popular topic in robot audition [1, 2, 3]. ASM aims at building a map of the respective locations of acoustic sources present in the environment of a robotic agent. It is closely related to simultaneous localization and mapping (SLAM) which is an extensively investigated and still actively developed framework in robotics. The need for applying SLAM-based methods arises through the fact that a mobile robotic agent can move within the environment, but is not able to directly observe its position. Hence, it must rely on direction-of-arrival (DoA) estimates obtained from the recorded microphone signals. A notable restriction of DoA observations is the fact, that they only convey information about the relative angle between the agent's heading direction and the observed sound sources. This is generally termed a bearing-only SLAM problem, as distance measurements cannot be obtained in this case. However, efficient algorithms have been proposed to tackle this problem by exploiting the agent's motion to build a map through triangulation [4].

An important aspect of the map building process is the maximization of the agent's knowledge about the environment. In the case of ASM, this refers to a reduction in uncertainty about the estimated source locations through movements of the robotic agent. It is especially important when using bearing-only sensors, as effective motion trajectories have to be obtained to optimally support the triangulation procedure. Implementations of SLAM algorithms usually rely on a recursive Bayesian estimation framework and represent the map as a probability distribution over source positions and the agent's pose [5, 6]. This allows to directly obtain a measure of uncertainty from the underlying probability density function (PDF).

Recent studies have proposed feedback strategies, which aim at generating motion controls for the robotic agent to minimize the uncertainty of the map. For instance, an information-based one-step-look-ahead control scheme for binaural localization was introduced in [7] and extended in [8]. It selects the next movement action in order to maximize the expected information gain between two consecutive time-steps. A similar approach based on Monte Carlo exploration (MCE) has been introduced in [9], where the expected information gain was predicted using Monte Carlo simulations inspired by the general framework presented in [10, Chap. 17]. Additionally, these methods have recently been extended towards multi-step ahead prediction and control in [11]. However, the described approaches do not consider the full SLAM problem, as they assume that the agent's pose is known or can be observed through other modalities. Related work without explicit knowledge of the agent's pose has been conducted outside the field of acoustic localization, e.g. in [12] for laser-based SLAM.

This study considers the full acoustic SLAM problem in the context of ASM. In contrast to previously proposed approaches using the FastSLAM [1] algorithm or Gaussian mixture probability hypothesis density (PHD) filters [2], the framework presented here is based on the inverse depth parametrization (IDP) of the source state [13], which allows an undelayed initialization of detected sources from bearing-only observations and computationally efficient recursive updates using an Unscented Kalman filter (UKF) [14]. A feedback control strategy based on the potential field (PF) method [15, 16] is proposed, which generates control inputs signals based on attractive and repulsive potential functions. The original method, which was developed in the context of path planning, navigation and obstacle avoidance, is adapted here to the task of active exploration. Therefore, task-specific forms of attractive and repulsive potentials are introduced based on the uncertainty minimization principle. They allow to generate trajectories supporting the triangulation capabilities of the robotic agent by simultaneously keeping safe distances towards mapped sources.

This paper is organzied as follows: Sec. 2 presents the acoustic SLAM model used in this study and describes the specific challenges of this method when using bearing-only acoustic measurements. Sec. 3 introduces the proposed active exploration policy based on the PF method and outlines the process of trajectory generation from attractive and repulsive potential functions. Sec. 4 compares the proposed approach to previously introduced methods in simulated acoustic scenarios, followed by the conclusions.

2. ACOUSTIC SLAM MODEL

The acoustic SLAM model introduced in this study is based on the general UKF-SLAM framework used for monocular vision [17]. At each discrete time-step k, estimates of current robot pose $\boldsymbol{r}_k$ and the acoustic scene map $\boldsymbol{s}$, have to be updated using their estimates from the previous time-step, observed DoA measurements $\boldsymbol{y}_k$ and control inputs $\boldsymbol{u}_k$. The scene map is considered to be time-invariant, implying that sound sources are not able to move within the environment. Hence, the discrete time index is omitted here. Extensions to dynamic acoustic scenes can be found in e.g. [3]. For a detailed introduction into the general framework of probabilistic SLAM, the reader is referred to [10, Chap. 10].

2.1. State space and system dynamics

The full state of the system is defined as $\boldsymbol{x}_k = \begin{bmatrix}\boldsymbol{r}_k & \boldsymbol{s}\end{bmatrix}^T$, where $\boldsymbol{r}_k = \begin{bmatrix}r_{\mathrm{x},k} & r_{\mathrm{y},k} & r_{\theta,k}\end{bmatrix}^T$ denotes the robot's pose at Cartesian coordinates $\{r_{\mathrm{x},k},\, r_{\mathrm{y},k}\}$ with heading direction $r_{\theta,k}$, while $\boldsymbol{s} = \begin{bmatrix}\boldsymbol{s}_1^T & \cdots & \boldsymbol{s}_N^T\end{bmatrix}^T$ models the acoustic scene map, represented by $n = 1, \ldots, N$ source states $\boldsymbol{s}_n$. In bearing-only SLAM, it is not possible to obtain an initial estimate of the Cartesian source position from only one set of DoA measurements. A delayed estimate could be obtained using several measurements from consecutive time-steps. However, due to measurement noise and association ambiguities, delayed initialization is generally considered a problematic approach in the context of bearing-only SLAM. Therefore, an alternative source state representation based on an IDP was proposed in [13], which is adopted here. Each source is modeled by a 4-dimensional state vector $\boldsymbol{s}_n = \begin{bmatrix}r_{\mathrm{x}_0,n} & r_{\mathrm{y}_0,n} & \rho_n & \alpha_n\end{bmatrix}^T$, where $r_{\mathrm{x}_0,n}$ and $r_{\mathrm{y}_0,n}$ are the Cartesian coordinates of the robot at the time of initialization, while ρ_n and α_n represent the inverse distance and relative angle towards the Cartesian position of the source, respectively. The notion of an inverse distance is adopted here, to yield a state variable that is bounded in $\rho_n \in [0,\, \frac{1}{d_{\min}}]$, where $d_{\min}$ is a fixed minimum distance towards the source location. The actual location of the n-th source can be obtained from the source state as

$$\boldsymbol{m}_n = \begin{bmatrix}m_{\mathrm{x},n}\\ m_{\mathrm{y},n}\end{bmatrix} = \begin{bmatrix}r_{\mathrm{x}_0,n}\\ r_{\mathrm{y}_0,n}\end{bmatrix} + \frac{1}{\rho_n}\begin{bmatrix}\cos(\alpha_n)\\ \sin(\alpha_n)\end{bmatrix} \qquad (1)$$

in 2-dimensional Cartesian map space $\boldsymbol{m}_n \in \mathbb{R}^2$ which is assumed in this study. It should be noted that an extension to three dimensions is straightforward (see e.g. [2]).

The dynamics of the robot's pose are governed by a two-wheel differential drive motion model [18] according to the nonlinear Gaussian process equation $\boldsymbol{r}_k = f(\boldsymbol{r}_{k-1},\, \boldsymbol{u}_k) + \boldsymbol{v}_k$, with

$$f(\boldsymbol{r}_{k-1},\, \boldsymbol{u}_k) = \begin{bmatrix} r_{\mathrm{x},k-1} + \frac{T_\mathrm{s}}{2}(u_{\mathrm{R},k} + u_{\mathrm{L},k})\cos(r_{\theta,k-1})\\ r_{\mathrm{y},k-1} + \frac{T_\mathrm{s}}{2}(u_{\mathrm{R},k} + u_{\mathrm{L},k})\sin(r_{\theta,k-1})\\ r_{\theta,k-1} + \frac{T_\mathrm{s}}{d_\mathrm{w}}(u_{\mathrm{R},k} - u_{\mathrm{L},k}) \end{bmatrix}, \qquad (2)$$

where T_s is the time between two consecutive discrete time-steps, $\boldsymbol{v}_k \sim \mathcal{N}(\boldsymbol{0},\, \boldsymbol{Q}_k)$ represents zero-mean Gaussian process noise with covariance matrix $\boldsymbol{Q}_k$, $\boldsymbol{u}_k = \begin{bmatrix}u_{\mathrm{R},k} & u_{\mathrm{L},k}\end{bmatrix}^T$ is the applied control input representing the angular wheel velocities of the right and left wheel and d_W is the spacing between the two actuated wheels.

2.2. Measurement model

Let $\boldsymbol{y}_k$ be an observation vector containing a set of DoA measurements at the k-th time-step. Following the IDP approach discussed in Sec. 2.1, the measurement model corresponding to the DoA of the n-th sound source can be expressed as a nonlinear Gaussian measurement equation $y_{n,k} = h(\boldsymbol{r}_k,\, \boldsymbol{s}_n) + \boldsymbol{w}_k$, with

$$h(\boldsymbol{r}_k,\, \boldsymbol{s}_n) = \operatorname{atan2}\Big(\frac{m_{\mathrm{y},n} - r_{\mathrm{y},k}}{m_{\mathrm{x},n} - r_{\mathrm{x},k}}\Big) - r_{\theta,k}, \qquad (3)$$

where $\boldsymbol{w}_k \sim \mathcal{N}(\boldsymbol{0},\, \boldsymbol{R}_k)$ represents zero-mean Gaussian measurement noise with covariance matrix $\boldsymbol{R}_k$. By exploiting the relation between the Cartesian source position $\boldsymbol{m}_n$ and the corresponding source state $\boldsymbol{s}_n$ given in Eq. (1), the measurement equation can be expressed as

$$h(\boldsymbol{r}_k,\, \boldsymbol{s}_n) = \operatorname{atan2}\Big(\frac{r_{\mathrm{y}_0,n} - r_{\mathrm{y},k} + \frac{1}{\rho_n}\sin(\alpha_n)}{r_{\mathrm{x}_0,n} - r_{\mathrm{x},k} + \frac{1}{\rho_n}\cos(\alpha_n)}\Big) - r_{\theta,k}, \qquad (4)$$

which can be applied directly in the state estimation framework that will be outlined in Sec. 2.4.

2.3. Map management

To obtain an accurate mapping of the acoustic scene, the estimated map state has to be constantly monitored and updated. Two important steps in this map management process are the initialization of newly detected sources in the map and the deletion of spurious sources caused by measurement errors.

If an observed DoA cannot be assigned to an already mapped source, it is considered as a candidate for extending the map state space $\boldsymbol{s}$ with a new source $\boldsymbol{s}_{N+1}$. Therefore, an initial source state has to be obtained from the measured DoA. As the distance cannot be observed from the acoustic signal, a direct initialization of the Cartesian source position is not possible. However, the IDP used here provides a means to achieve undelayed initialization, even without explicit distance information. For a detailed description of the initialization procedure using IDP, cf. [13]. The deletion of unreliable source estimates and outliers due to spurious measurements is handled using the log-odds ratio method described in [19].

2.4. State estimation

The system state is recursively estimated at each time-step using a generic UKF framework. Many SLAM methods which do not use acoustic signals as observations rely on the extended Kalman filter (EKF) because of its reduced computational complexity compared to the UKF [20]. This is especially useful when dealing with a huge number of landmarks, e.g. in the context of laser or vision-based SLAM. However, the number of sources in an acoustic scene is usually limited, resulting in a rather small estimation state-space. Therefore, the UKF is used here due to its more accurate estimation capabilities in the presence of nonlinearities [14].

3. POTENTIAL-FIELD-BASED EXPLORATION

The PF method was introduced in [15] for robotic path planning and obstacle avoidance. It is based on an artificial PF imposed on the robot's environmental map, which directs the robot to a specific goal position by computing the gradient of this field. Herein, the goal position is defined as an attractive force or minimum, whereas obstacles act as repulsive forces, represented as peaks in the field. By superimposing all artificial forces that influence the robot, a smooth trajectory towards the goal position can be obtained.

3.1. Potential functions

Let $U(\boldsymbol{q}_k) = U_\mathrm{a}(\boldsymbol{q}_k,\, n) + U_\mathrm{r}(\boldsymbol{q}_k)$ be a differentiable potential function with corresponding gradient $F(\boldsymbol{q}_k) = -\nabla U(\boldsymbol{q}_k)$ in Cartesian map space $\boldsymbol{q}_k \in \mathbb{R}^2$. Following the general approach from [15], the potential function is composed of an attractive potential and a repulsive potential. The attractive potential is specified as

$$U_\mathrm{a}(\boldsymbol{q}_k,\, n) = \frac{\beta_\mathrm{a}}{2} d_n^2(\boldsymbol{q}_k), \tag{5}$$

where $d_n(\boldsymbol{q}_k) = \|\boldsymbol{q}_k - \boldsymbol{m}_n\|$ models the Euclidean distance to the position of the n-th source in the map and β_a is a scaling factor.

The conventional PF method assumes that a dedicated goal position for a specific navigation task is defined by the attractive potential. In contrast, this study considers active exploration where the target is the position of a mapped sound source. This notion is inspired by the fact that acoustic localization in reverberant conditions benefits if the acoustic sensors are placed within the critical distance of the source [21]. Therefore, a greedy goal-selection policy $U_\mathrm{a}(\boldsymbol{q}_k,\, n^\star)$ is introduced here, which chooses the mapped source with the highest uncertainty as goal, according to $n^\star = \arg\max_n H(\boldsymbol{s}_n)$, where $H(\boldsymbol{s}_n)$ is the entropy associated with the n-th source state. The UKF state estimation framework described in Sec. 2.4 assumes a multivariate Gaussian PDF. Therefore, the required entropies can be computed analytically as $H(\boldsymbol{s}_n) = \frac{1}{2}\log(|2\pi e \boldsymbol{\Sigma}_{n,k}|)$, where $\boldsymbol{\Sigma}_{n,k}$ represents the covariance matrix of the n-th source state posterior.

The definition of the repulsive potential differs from its original formulation [15] and is adapted to the specific requirements for active exploration in this study. Generally, each source position should apply a repulsive force on the robot to avoid collisions. However, in the context of active exploration, repulsive potentials can also be used to steer the robot on specific trajectories that support its localization capabilities. This is especially beneficial for bearing-only SLAM requiring triangulation to estimate distance. An optimal trajectory for this task is a perfect circle around the source, which maintains a constant distance but achieves changes in relative azimuth at each time-step, which is beneficial for triangulation [7, 8, 9]. Therefore, a repulsive potential is proposed here, which explicitly considers two aspects: maintaining a safe distance and simultaneously rewarding circular trajectories around all mapped sources. It is defined as $U_\mathrm{r}(\boldsymbol{q}_k) = U_{\mathrm{r}_1}(\boldsymbol{q}_k) + U_{\mathrm{r}_2}(\boldsymbol{q}_k)$ with

$$U_{\mathrm{r}_1}(\boldsymbol{q}_k) = \frac{\beta_{\mathrm{r}_1}}{2}\sum_{n=1}^{N}\begin{cases}\left(\frac{1}{d_n(\boldsymbol{q}_k)} - \frac{1}{d_0}\right)^2 & \text{if } d_n(\boldsymbol{q}_k) \le d_0\\ 0 & \text{if } d_n(\boldsymbol{q}_k) > d_0\end{cases} \tag{6}$$

and

$$U_{\mathrm{r}_2}(\boldsymbol{q}_k) = \frac{\beta_{\mathrm{r}_2}}{2}\sum_{n=1}^{N}\left[1 - \cos\left(\phi_n(\boldsymbol{q}_k) - \frac{\pi}{2}\right)^2\right], \tag{7}$$

where β_{r_1} and β_{r_2} are scaling factors, d_0 is the minimum distance that should be kept towards a source and $\phi_n(\boldsymbol{q}_k)$ represents the relative angle towards the n-th source in the map. It should be noted that this kind of repulsive potential is similar to the extended PF method introduced in [15], where angle-dependent potential functions were used for improved collision avoidance. In contrast to the attractive potential, the repulsive potential is computed considering all mapped sources to avoid collisions according to the safe distance criterion.

3.2. Control signal generation

Control signals are generated based on trajectories that follow the steepest descent along the gradient of the potential function. Similar to the original formulation of the PF method [15], this gradient can be expressed as a superposition of attractive and repulsive forces $F_\mathrm{a}(\boldsymbol{q}_k,\, n) = -\nabla U_\mathrm{a}(\boldsymbol{q}_k,\, n)$ and $F_\mathrm{r}(\boldsymbol{q}_k) = -\nabla U_\mathrm{r}(\boldsymbol{q}_k)$, respectively. For the proposed greedy exploration policy, this yields the attractive force

$$F_\mathrm{a}(\boldsymbol{q}_k,\, n^\star) = -\beta_\mathrm{a}(\boldsymbol{q}_k - \boldsymbol{m}_{n^\star}) \tag{8}$$

based on Eq. (5) and the corresponding repulsive forces

$$F_{\mathrm{r}_1}(\boldsymbol{q}_k) = \beta_{\mathrm{r}_1}\sum_{n=1}^{N}\begin{cases}\left(\frac{1}{d_n(\boldsymbol{q}_k)} - \frac{1}{d_0}\right)\frac{\boldsymbol{q}_k - \boldsymbol{m}_n}{d_n^3(\boldsymbol{q}_k)} & \text{if } d_n(\boldsymbol{q}_k) \le d_0\\ 0 & \text{if } d_n(\boldsymbol{q}_k) > d_0\end{cases} \tag{9}$$

and

$$F_{\mathrm{r}_2}(\boldsymbol{q}_k) = -\beta_{\mathrm{r}_2}\sum_{n=1}^{N}\sin\left(\phi_n(\boldsymbol{q}_k) - \frac{\pi}{2}\right)\nabla\phi_n(\boldsymbol{q}_k), \tag{10}$$

where $\nabla\phi_n(\boldsymbol{q}_k)$ is the gradient of the inverse tangent function, which is omitted here due to space limitations (see e.g. [10, Chap. 7]). Corresponding motion trajectories can directly be obtained from the superimposed attractive and repulsive forces by following a path of steepest descent along the gradient towards a minimum.

However, the conventional PF method can be problematic in cases with several local minima in trajectory space, where the robotic agent might get stuck in a local minimum without being able to reach the target position [16]. The modified approach presented here circumvents this problem, because active exploration is inherently an online approach which requires constant updates of the potential functions and their corresponding forces. Therefore, the robotic agent has to frequently re-plan its trajectory, reducing the risk of getting stuck in a local minimum during exploratory movements.

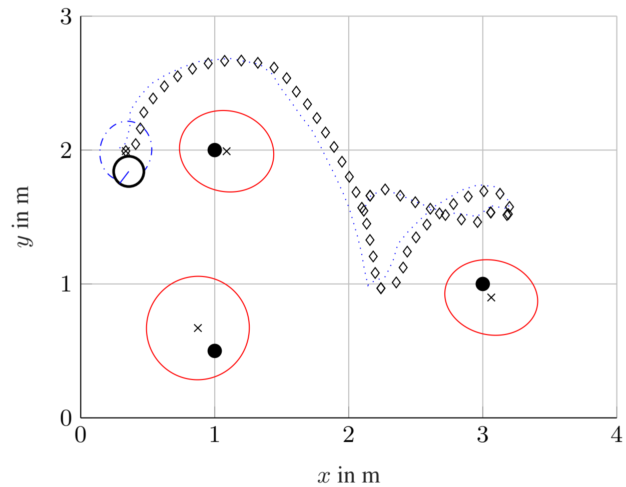

Fig. 1: Exemplary trajectory generated by the proposed PF-based approach. Thick black dots show the ground-truth sound source positions and crosses surrounded by solid red ellipses represent the estimated source positions with corresponding 95% confidence intervals. The uncertainty of the robot's pose is depicted as the dashed, blue 95% confidence interval ellipse. The dotted blue line is the ground-truth robot path, whereas the estimated robot positions are shown as diamond symbols at each time-step. The initial pose of the robot was set to $\boldsymbol{r}_0 = [2 \quad 1.5 \quad 0]^T$.

Table 1: Monte Carlo simulation results. Localization gross accuracies A_{L} and F_1 scores are shown in percentage values between zero and one, localization fine-errors $E_{\mathrm{L,f}}$ and translational pose errors $E_{\mathrm{P,t}}$ are given in meters and rotational pose errors $E_{\mathrm{P,r}}$ in degrees.

T_{60}	Anechoic					0.5 s					1 s				
	A_{L}	F_1	$E_{\mathrm{L,f}}$	$E_{\mathrm{P,t}}$	$E_{\mathrm{P,r}}$	A_{L}	F_1	$E_{\mathrm{L,f}}$	$E_{\mathrm{P,t}}$	$E_{\mathrm{P,r}}$	A_{L}	F_1	$E_{\mathrm{L,f}}$	$E_{\mathrm{P,t}}$	$E_{\mathrm{P,r}}$
IBF [8]	0.79	0.75	0.50	**0.31**	1.07	0.78	0.70	0.51	**0.32**	1.13	0.74	0.65	0.49	0.33	1.10
MCE [9]	0.78	0.68	0.52	0.33	1.02	0.73	0.63	**0.49**	0.33	1.10	0.63	0.57	0.51	0.79	1.17
Proposed	**0.86**	**0.79**	**0.47**	**0.31**	**1.01**	**0.83**	**0.75**	**0.49**	**0.32**	**1.02**	**0.78**	**0.70**	**0.47**	**0.32**	**1.03**

Furthermore, the dependence of the repulsive force on the relative angles towards all sources in the map results in a smoother optimization surface in trajectory space, compared to the conventional PF method where this is not explicitly considered. The benefit of this for conventional path planning has also been reported in [15, 22]. Throughout all experiments that were conducted in this study, problems resulting from local minima have never been observed. An example of a trajectory obtained with the proposed approach is depicted in Fig. 1.

4. EVALUATION

The performance of the proposed approach was evaluated in simulated reverberant acoustic scenarios. As a baseline, the active exploration methods based on information-based feedback (IBF) [7] and MCE [9] were chosen for comparison.

4.1. Experimental setup

Monte Carlo simulations were conducted in a simulated "shoebox"-shaped room of size $5\,\mathrm{m} \times 4\,\mathrm{m} \times 3\,\mathrm{m}$ for three different reverberation times T_{60} of $0\,\mathrm{s}$ (anechoic), $0.5\,\mathrm{s}$ and $1\,\mathrm{s}$. An array of four microphones was employed as the acoustic sensor. The microphone placement on the robotic agent was selected according to the array configuration of the humanoid robot NAO [23]. For each simulation, an acoustic scene with three sound sources emitting speech signals obtained from the GRID audiovisual corpus [24] was rendered using the image-source method [25]. The positions of the sound sources, as well as their activity periods were varied during each simulation. The initial position of the robotic agent was always set to the center of the room. Each experiment consisted of 250 Monte Carlo simulations. The motion dynamics of the robotic agent were simulated using the kinematic model (2) introduced in Sec. 2.1 with Gaussian noise. DoA measurements were obtained using the multiple signal classification (MUSIC) algorithm [26] for multi-source localization. The scaling parameters of the proposed PF approach were set to $\beta_{\mathrm{a}} = 10$, $\beta_{\mathrm{r}_1} = 1$ and $\beta_{\mathrm{r}_2} = 1000$, respectively. The minimum distance was set to $d_0 = 0.5\,\mathrm{m}$.

4.2. Evaluation metrics

During each simulation, a source was assumed to be detected when the estimated position lies within a $1\,\mathrm{m}$ radius around the corresponding ground-truth position. Localization performance was evaluated based on gross accuracy A_{L} and fine-error $E_{\mathrm{L,f}}$ similar to [27], where gross accuracy is defined as the percentage of detected sources and fine error measures the average of localization error for all detected sources during a simulation. Additionally, the F_1 score is reported to reflect the effects of false positive source detections. For evaluating full SLAM performance, translational ($E_{\mathrm{P,t}}$) and rotational ($E_{\mathrm{P,r}}$) pose errors were obtained by averaging the errors between the estimated and ground-truth robot trajectories. To evaluate the computational performance of all control methods, the required average computation times T_{c} were estimated by averaging the time needed for computing the control input signal at each time-step.

Table 2: Average computation time T_{c} for all evaluated methods in ms. Experiments were conducted in MATLAB on an INTEL® Core™ i5 machine with 16 GB RAM running Ubuntu 16.04.

	IBF [8]	MCE [9]	Proposed
T_{c}	8.73	57.26	**0.09**

4.3. Results and discussion

The results in Tab. 1 show that the proposed approach outperforms both baseline methods in gross accuracy and F_1 score for all considered acoustic conditions. The achieved improvements are statistically significant according to a t-test with $p < 0.05$. Additionally, the achieved localization fine-error of the proposed approach is considerably lower compared to the baseline in all conditions. It has to be noted, that for SLAM, gross accuracy and F_1 score are the most important measures, as undetected sources bear a risk for collision. In contrast, the self-localization performance of the robotic agent does not seem to be affected much by the choice of the control method. The experiments have shown that it is generally sufficient for self-localization if one source has been correctly detected and localized. The DoA estimation via MUSIC which is adopted here, has been proven to yield accurate estimates even in challenging reverberant conditions. This explains the insignificant differences in pose error between all methods.

Tab. 2 shows that the proposed method outperforms both baseline methods in terms of the required computation time. This can be explained by the fact that computationally expensive predictions or Monte Carlo simulations are not required for generating control signals for the next time-step.

5. CONCLUSION

This study proposed an active exploration strategy based on the potential field method for acoustic SLAM. The bearing-only problem arising from the use of DoA measurements was solved by a state-space model based on the inverse depth parametrization in a recursive Bayesian estimation framework using an unscented Kalman filter. An experimental evaluation in simulated acoustic conditions has shown that the proposed approach clearly outperforms recently introduced methods for this task in terms of acoustic scene mapping performance and simultaneously leads to a greatly reduced computational complexity. This makes the proposed approach especially appealing for real-time applications on physical robotic systems.

6. REFERENCES

[1] J.-S. Hu, C.-Y. Chan, C.-K. Wang, M.-T. Lee, and C.-Y. Kuo, "Simultaneous Localization of a Mobile Robot and Multiple Sound Sources Using a Microphone Array," *Advanced Robotics*, vol. 25, no. 1-2, pp. 135–152, 2011.

[2] C. Evers, A. H. Moore, and P. A. Naylor, "Acoustic simultaneous localization and mapping (A-SLAM) of a moving microphone array and its surrounding speakers," in *2016 IEEE International Conference on Acoustics, Speech and Signal Processing (ICASSP)*, March 2016, pp. 6–10.

[3] C. Evers, Y. Dorfan, S. Gannot, and P. A. Naylor, "Source tracking using moving microphone arrays for robot audition," in *2017 IEEE International Conference on Acoustics, Speech and Signal Processing (ICASSP)*, March 2017, pp. 6145–6149.

[4] K. E. Bekris, M. Glick, and L. E. Kavraki, "Evaluation of algorithms for bearing-only SLAM," in *2006 IEEE International Conference on Robotics and Automation (ICRA)*, May 2006.

[5] H. Durrant-Whyte and T. Bailey, "Simultaneous Localization and Mapping: Part I," *IEEE Robotics Automation Magazine*, vol. 13, no. 2, pp. 99–110, June 2006.

[6] T. Bailey and H. Durrant-Whyte, "Simultaneous Localization and Mapping: Part II," *IEEE Robotics Automation Magazine*, vol. 13, no. 3, pp. 108–117, Sept 2006.

[7] G. Bustamante, A. Portello, and P. Danès, "A three-stage framework to active source localization from a binaural head," in *2015 IEEE International Conference on Acoustics, Speech and Signal Processing (ICASSP)*, April 2015, pp. 5620–5624.

[8] G. Bustamante, P. Danès, T. Forgue, and A. Podlubne, "Towards information-based feedback control for binaural active localization," in *2016 IEEE International Conference on Acoustics, Speech and Signal Processing (ICASSP)*, March 2016, pp. 6325–6329.

[9] C. Schymura, J. D. Rios Grajales, and D. Kolossa, "Monte Carlo exploration for active binaural localization," in *2017 IEEE International Conference on Acoustics, Speech and Signal Processing (ICASSP)*, March 2017.

[10] S. Thrun, W. Burgard, and D. Fox, *Probabilistic Robotics*, The MIT Press, 2005.

[11] Q. V. Nguyen, F. Colas, E. Vincent, and F. Charpillet, "Long-term robot motion planning for active sound source localization with Monte Carlo tree search," in *2017 Hands-free Speech Communications and Microphone Arrays (HSCMA)*, March 2017, pp. 61–65.

[12] F. Bourgault, A. A. Makarenko, S. B. Williams, B. Grocholsky, and H. F. Durrant-Whyte, "Information based adaptive robotic exploration," in *IEEE/RSJ International Conference on Intelligent Robots and Systems*, 2002, pp. 540–545.

[13] J. Civera, A. J. Davison, and J. M. M. Montiel, "Inverse Depth Parametrization for Monocular SLAM," *IEEE Transactions on Robotics*, vol. 24, no. 5, pp. 932–945, October 2008.

[14] S. J. Julier and J. K. Uhlmann, "A new extension of the Kalman filter to nonlinear systems," in *Proc. of AeroSense: The 11th Int. Symp. on Aerospace/Defence Sensing, Simulation and Controls*, July 1997.

[15] O. Khatib, *The Potential Field Approach And Operational Space Formulation In Robot Control*, pp. 367–377, Springer US, Boston, MA, 1986.

[16] Y. Koren and J. Borenstein, "Potential field methods and their inherent limitations for mobile robot navigation," in *1991 IEEE International Conference on Robotics and Automation (ICRA)*, April 1991, pp. 1398–1404.

[17] S. A. Holmes, G. Klein, and D. W. Murray, "An $\mathcal{O}(N^2)$ Square Root Unscented Kalman Filter for Visual Simultaneous Localization and Mapping," *IEEE Transactions on Pattern Analysis and Machine Intelligence*, vol. 31, no. 7, pp. 1251–1263, July 2009.

[18] E. Maulana, M. A. Muslim, and A. Zainuri, "Inverse kinematics of a two-wheeled differential drive an autonomous mobile robot," in *2014 Electrical Power, Electronics, Communicatons, Control and Informatics Seminar (EECCIS)*, Aug 2014, pp. 93–98.

[19] M. Montemerlo and S. Thrun, "Simultaneous localization and mapping with unknown data association using FastSLAM," in *2003 IEEE International Conference on Robotics and Automation*, Sept 2003, vol. 2, pp. 1985–1991.

[20] Z. Kurt-Yavuz and S. Yavuz, "A comparison of EKF, UKF, FastSLAM2.0, and UKF-based FastSLAM algorithms," in *2012 IEEE 16th International Conference on Intelligent Engineering Systems (INES)*, June 2012, pp. 37–43.

[21] E. Georganti, T. May, S. van de Par, and J. Mourjopoulos, "Sound source distance estimation in rooms based on statistical properties of binaural signals," *IEEE Transactions on Audio, Speech, and Language Processing*, vol. 21, no. 8, pp. 1727–1741, Aug 2013.

[22] R. Siegwart, I. R. Nourbakhsh, and D. Scaramuzza, *Introduction to Autonomous Mobile Robots*, The MIT Press, 2nd edition, 2011.

[23] Aldebaran Robotics, *NAO Humanoid Robot Platform Datasheet*, 2012, `https://www.ald.softbankrobotics.com/sites/aldebaran/files/datasheet_nao_next_gen_en.pdf`.

[24] M. Cooke, J. Barker, S. Cunningham, and X. Shao, "An audio-visual corpus for speech perception and automatic speech recognition," *The Journal of the Acoustical Society of America*, vol. 120, no. 5, pp. 2421–2424, 2006.

[25] J. B. Allen and D. A. Berkley, "Image method for efficiently simulating small-room acoustics," *The Journal of the Acoustical Society of America*, vol. 65, no. 4, pp. 943–950, 1979.

[26] C. T. Ishi, O. Chatot, H. Ishiguro, and N. Hagita, "Evaluation of a MUSIC-based real-time sound localization of multiple sound sources in real noisy environments," in *2009 IEEE/RSJ International Conference on Intelligent Robots and Systems*, October 2009, pp. 2027–2032.

[27] J. Woodruff and D. Wang, "Binaural localization of multiple sources in reverberant and noisy environments," *IEEE Transactions on Audio, Speech, and Language Processing*, vol. 20, no. 5, pp. 1503–1512, July 2012.